Effects of driver direct visibility in passenger vehicles on the risk of turning crashes with pedestrians

November 2025

Wen Hu
Jessica B. Cicchino

Insurance Institute for Highway Safety
4121 Wilson Boulevard, 6th floor
Arlington, VA 22203
researchpapers@iihs.org
+1 703 247 1500

iihs.org

Contents

ABSTRACT

Introduction: This study examined if characteristics of direct visibility metrics in passenger vehicles, such as large blind zones, corresponded with being overrepresented in left- and right-turning crashes with pedestrians. It also evaluated the effects of vehicle front structures on some direct visibility metrics.

Method: The analysis included single-passenger vehicle, single-pedestrian crashes in seven states. Direct visibility metrics used in the crash analysis included driver- and passenger-side blind zone sizes, front nearest visible point (NVP) distance, and front field of view (FOV) width. The blind zone sizes and front NVP distances were measured by using a camera-based method, which captured obscuration produced by all vehicle front structures. The front FOV width was measured at a driver's eye-height horizon by using a laser measuring tool. Direct visibility measurements were taken on 168 unique combinations of vehicle make, series, and redesign years. Logistic regression analyses were performed to evaluate the effects of visibility metrics and other factors on the odds of a left- or right-turning pedestrian crash relative to a straight-moving pedestrian crash. Additionally, linear regression analyses were performed to examine the effects of front-structure geometries on blind zone sizes and front NVP distances.

Results: For left-turning pedestrian crashes relative to straight-moving pedestrian crashes, when compared with a small driver-side blind-zone size (≤ 20%), a large (> 30%) and a medium (> 20% and ≤ 30%) size were respectively associated with a significant 69.7% and 59.0% increase in the odds. A small (≤ 85°) and a medium (> 85° and ≤ 90°) front FOV width were associated with significant increases of 50.8% and 18.2% in the odds, respectively, compared with a large front FOV width (> 90°). A long front NVP distance (> 9 m) was associated with a significant 36.8% increase in the odds, and a medium distance (> 6 and ≤ 9 m) was associated with a nonsignificant 9.8% increase in the odds, compared with a short distance (≤ 6 m). No significant effects of direct visibility metrics were found on the risk of right-turning pedestrian crashes.

Conclusions: Larger driver-side blind zones, longer front NVP distances, and narrower front FOVs were associated with increased risk of left-turning pedestrian crashes. The study also validated the effects of vehicle front structures including A-pillars, side mirrors, hoods, and windshields on blind zone sizes and front NVP distances.

Practical applications: Findings could help automakers improve safety for road users outside vehicles with changes in vehicle design to enhance drivers' direct vision and improvements to automatic-emergency-breaking technology to address vehicle-turning conflicts.

Keywords: direct visibility, passenger vehicles, pedestrian crashes, turning vehicles, blind zone, front nearest visible point (NVP) distance, front field of view (FOV)

1. INTRODUCTION

Pedestrians represent a considerable portion of motor-vehicle crash injuries and deaths in the United States. In 2023, a total of 7,314 pedestrians were killed, which was an 78% increase from its lowest point in 2009, and approximately 67,000 pedestrians were injured (Insurance Institute for Highway Safety [IIHS], 2025). Between 2013 and 2022, pedestrian death rates increased 50% in the Unites States, while they generally declined in other high-income countries (Naumann et al., 2025).

Addressing pedestrian safety requires a Safe System approach that creates redundancies by implementing countermeasures applying to roads, people, and vehicles. While many engineering and enforcement countermeasures have been proven effective in improving pedestrian safety by increasing pedestrian visibility, separating pedestrians from vehicular traffic, and reducing vehicle speeds (Federal Highway Administration, 2023; Hu & Cicchino, 2020a, 2020b, 2024; Hu et al., 2025; Hu & McCartt, 2016; Rothman et al., 2015; Wilson et al., 2010), safe vehicles are an essential part of the system.

Vehicle characteristics impact pedestrian injury risk in motor-vehicle crashes as well as the risk of certain types of pedestrian crashes. Light truck vehicles (LTVs) such as SUVs and pickups are associated with higher risk of severe or fatal injuries to pedestrians when compared with cars (Ballesteros et al., 2004; Edwards & Leonard, 2022; Lefler & Gabler, 2004; Longhitano et al., 2005; Monfort & Mueller, 2020; Paulozzi, 2005; Roudsari et al., 2005; Roudsari et al., 2004). Hu et al. (2024) found that vehicles with tall and/or blunt front ends, as observed in a majority of SUVs and pickups, were associated with higher pedestrian fatality risk. Tall and blunt front ends also increased pedestrian injury severity (Monfort et al., 2024). In terms of pedestrian crash types, LTVs were more likely than cars to strike pedestrians when turning or when pedestrians were on or near the edge of a travel lane (Hu & Cicchino, 2022). This finding pointed to the potentially problematic obscuration of the driver's view near the front corners of larger passenger vehicles, but since no known research has systematically examined driver visibility by passenger vehicle type, Hu and Cicchino (2022) could not conclusively determine why LTVs were overinvolved in these pedestrian crashes.

Among vehicle structures that produce blind zones to the front and side, A-pillars have been identified as an obstruction of drivers' field of view (Allen et al., 2001; Santos et al., 2020). Larger A-pillars increased the size of obscuration areas, and A-pillars closer to the forward line of sight moved blind zones closer to vehicle travel paths (Reed, 2008). Pedestrian crashes increased as A-pillar blind zones grew larger and declined as the horizontal field of view through the windshield widened (Ogawa et al., 2013). The shape of A-pillars matters too. Many vehicles have A-pillars that are broader at their base, leading to wide blind zones in areas where pedestrians may be present (Hussein et al., 2017). In addition to A-pillars, vehicle hoods and side mirrors may produce obscuration (Epstein et al., 2025; Mueller et al., 2025).

The size and location of surrounding environments that are invisible to drivers can be assessed by examining drivers' direct visibility, which measures the driver's ability to see surroundings directly through vehicle windows. Research on the relationship between crash risk to pedestrians and drivers' direct visibility to the front and side has been mainly focused on heavy trucks (Galal et al., 2024). Trucks with low direct vision were more likely to strike pedestrians than trucks with relatively high direct vision (Woolsgrove, 2014; Young et al., 2023). For passenger vehicles, Jagtap and Jermakian (2025) obtained the blind zone data of 20 passenger vehicles by using a method that measured driver direct visibility, and simulated interactions between crossing pedestrians and vehicle blind zones associated with A-pillars and side mirrors under various scenarios at intersections. The simulation results showed that pedestrians were frequently in blind zones during left-turning maneuvers, especially when they approached from the driver's side, and large blind zones delayed a pedestrian's exit from a blind zone, which would potentially reduce the time available for a driver to react to avoid a crash. No known study has examined the association between direct visibility of passenger vehicles and pedestrian crash risks by using real-world crash data.

This study aimed to examine whether larger blind zones and other direct visibility metrics were associated with higher risks of crashes between pedestrians and turning passenger vehicles. The analysis

used police-reported crash data and evaluated the relationship between turning crash risks and direct visibility metrics of passenger vehicles by comparing vehicle precrash movements (turning left vs. moving straight, turning right vs. moving straight). Direct visibility metrics were obtained by following a camera-based method that used photography to provide all-around visibility maps from all vehicle structures that blocked a driver's vision (Mueller et al., 2025). The second purpose of the study was to examine direct visibility characteristics by passenger vehicle type to provide insights into the increased risks of pedestrian crashes involving turning vehicles associated with LTVs. Thirdly, the study examined the effects of vehicle front structures including A-pillars, side mirrors, hoods, and windshields on some of the direct visibility metrics, which could help automakers improve vehicle design to enhance drivers' direct vision and safety of road users outside vehicles.

2. METHOD

2.1 Data

Data for this study were built upon the analysis data in Hu et al. (2024), which included police-reported pedestrian crash data and front-end-profile parameters of passenger vehicles involved in these crashes.

Crashes included in the current analysis involved a single passenger vehicle and a single pedestrian ages 16 years or older in seven states: Connecticut, Florida, Maryland, Michigan, New Jersey, Ohio, and Pennsylvania. Crash years were from 2017 to 2020 or 2021 depending on the states, which was the latest year for which crash data were available at the time of analysis by Hu et al. (2024). In addition to driver, pedestrian, and environmental information, crash data necessary for analysis such as speed limits, vehicle precrash movements, and impact points were available. Crashes were included in the current analysis if the vehicle was moving straight, turning left, or turning right prior to a crash, and its front, driver side, or passenger side struck a pedestrian.

When available, Vehicle Identification Numbers (VINs) of vehicles involved in these pedestrian crashes were decoded to obtain vehicle information by using VINDICATOR, a VIN-decoding program maintained by the Highway Loss Data Institute. Vehicle information obtained included passenger vehicle type; vehicle make, series, and model year; vehicle model redesign year; and the availability of pedestrian automatic emergency braking (AEB) systems. Only vehicles without pedestrian AEB systems were included in the analysis.

Front-end geometries of vehicles involved in pedestrian crashes were used in the analysis, including hood leading edge height, hood length, hood angle, and windshield angle, to examine their effects on drivers' direct visibility to the front and side. These geometries were measured by using ImageJ, a free image-analysis tool. A side-view photo of each vehicle was input into ImageJ, and front-end-profile parameters were manually labeled on the photo and measured. All measurements were calibrated using the vehicle's wheelbase. The detailed procedure was described in Hu et al. (2024).

2.2 Metrics of drivers' direct visibility

Direct visibility measurements were taken on 168 of the vehicles included in the Hu et al. (2024) data set that represented different vehicle make, series, and redesign years. A vehicle redesign year is a model year when a vehicle undergoes a major change from the previous version, typically including significant changes to the exterior design, interior layout, and so on. For the same vehicle make and series, the same measurements apply to all model years between redesign years. Measurements were taken in vehicle sales lots from December 2023 to May 2024. Not all the vehicles included in Hu et al. (2024) were measured in the current study due to difficulties locating some vehicles during the measurement time frame.

By following the camera-based method as described in Mueller et al. (2025) and in the *IIHS Driver Direct Visibility Protocol* (IIHS, 2024), 360-degree direct visibility maps of the nearest visible points (NVPs) at ground level were produced for vehicles. The ground areas between the vehicle and the NVPs were blind zones, and ground areas beyond the NVPs were visible to drivers (Figure 1). For each

passenger vehicle measured, visibility maps were created from the eye point of a 50th percentile male driver seated at a mid-track, mid-height position, and from the eye point of a 5th percentile female driver seated at a full-forward, full-up position. The height of a 50th percentile male is 176 cm, and the height of a 5th percentile female is 150 cm. The 50th percentile male driver measurements applied to a total of 766 unique combinations of vehicle make, series, and model year, which were involved in pedestrian crashes included in the analysis. The 5th percentile female driver measurements applied to fewer vehicles due to missing data: 728 combinations of vehicle make, series, and model year. The model years of these vehicles ranged from 1999 and 2021, with nearly 90% of them being older than 2019.

Direct visibility metrics used in this study included the percentage of the driver-side blind zone area in the quarter circle with an 18-m radius centered at the left front corner of a vehicle at ground level (referred to as driver-side blind zone size), and the percentage of the passenger-side blind zone area in the 30° sector with a 18-m radius centered at the same corner (referred to as the passenger-side blind zone size; Figure 1). For the passenger-side blind zone size, a central angle of 30° instead of 90° was used to calculate the percentage, since the 30° sector covered the blind zone mostly associated with the A-pillar and side mirror on the passenger side, while a 90° sector included too much of the blind zone in the front. An 18-m radius was selected, as it adequately captured the variations in the blind zone areas across vehicles. Additionally, mathematical simulations indicated that this distance of 18 m encompassed the paths of crossing pedestrians during left turns (Jagtap & Jermakian, 2025). Another direct visibility metric included was the front NVP distance, which was the distance between the camera eye location and the NVP in front of a vehicle at ground level (Figure 1).

Additionally by using a laser measuring tool (Mueller et al., 2025), driver- and passenger-side A-pillar widths (in degrees) at a driver's eye-height horizon (referred to as driver- and passenger-side A-pillar width) were measured, as well as the front field of view (FOV) width (in degrees) between the inner sides of A-pillars at a driver's eye-height horizon (Figure 2). The laser was projected horizontally (leveled

to ground) from the height of the driver's eyes. The side mirrors' maximum height and maximum width were measured at locations where the mirror was the tallest or the widest.

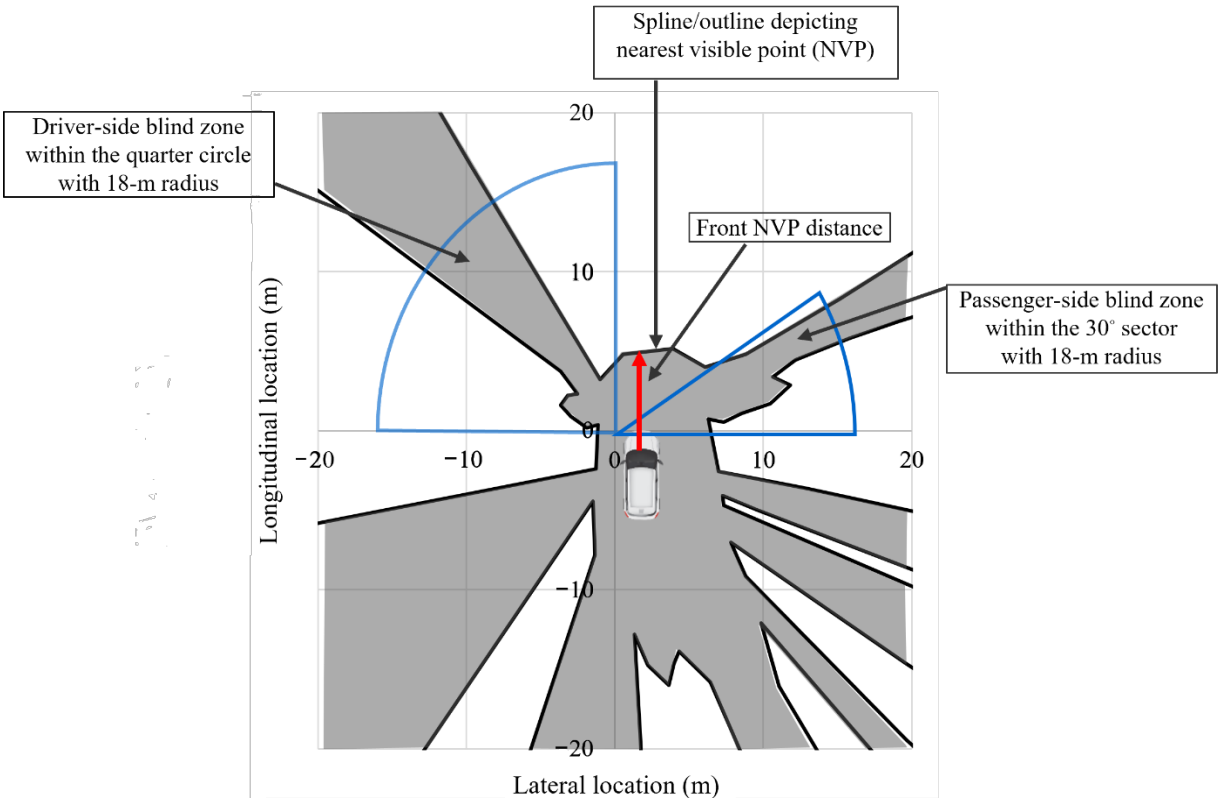

Figure 1. Driver- and passenger-side blind zones and front NVP distance using the camera-based perspective transformation method

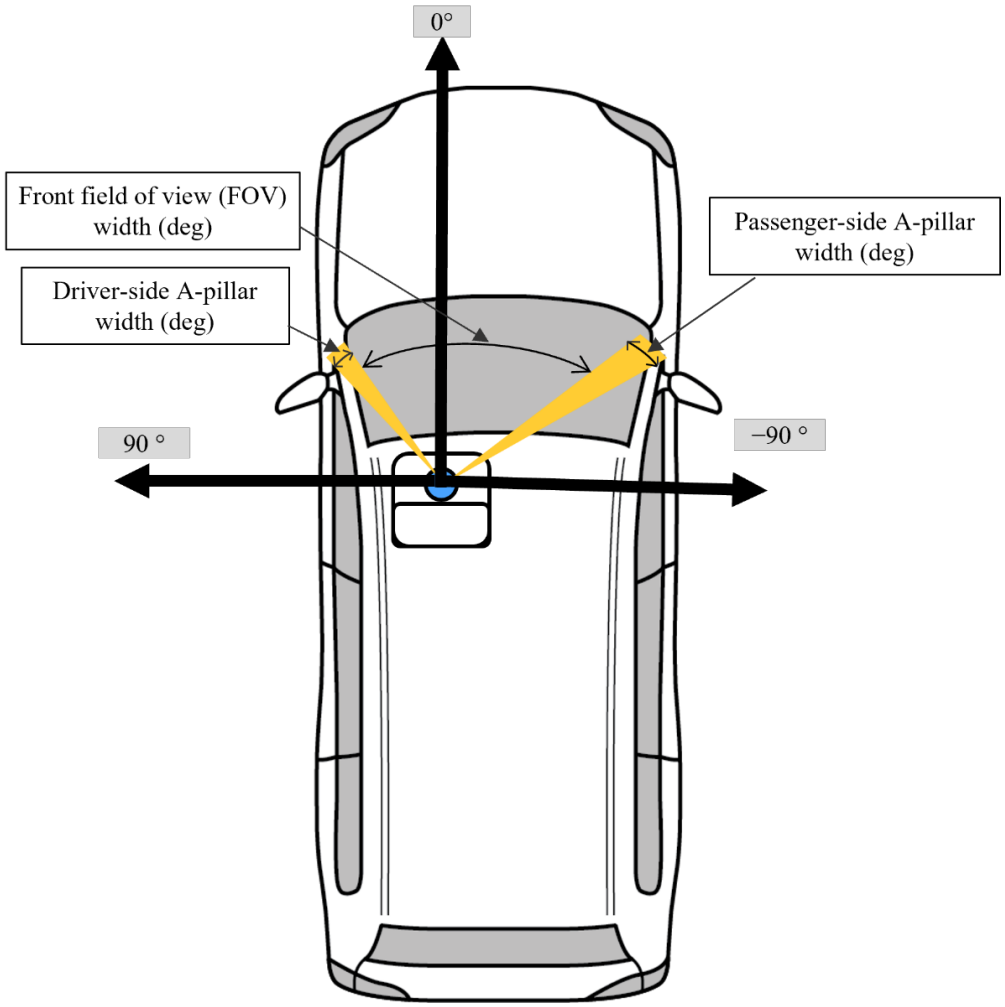

Figure 2. Measurements at a driver's eye-height horizon by using a laser measuring tool

2.3 Analyses

2.3.1 Association between direct visibility metrics and pedestrian crash types

The goal of the primary analyses was to determine if characteristics of direct visibility metrics for passenger vehicles such as larger blind zones are associated with increased risks of left- and right-turning crashes with pedestrians. Logistic regression analysis evaluated the effects of direct visibility metrics on the odds of crashes where a left-turning or a right-turning passenger vehicle strikes a pedestrian, relative to crashes where a straight-moving vehicle strikes a pedestrian, while controlling for other factors that might have affected crash types. In the remainder of this paper, these crash types are referred to as left-

turning pedestrian crashes, right-turning pedestrian crashes, and straight-moving pedestrian crashes. Separate analyses were performed for left-turning and right-turning pedestrian crashes. The 50th percentile male driver direct visibility measurements were used in the crash type analysis because they would be more representative of the height of average drivers than the 5th percentile female driver measurements.

The dependent variable was the crash type indicator (left-turning pedestrian crashes vs. straight-moving pedestrian crashes, right-turning pedestrian crashes vs. straight-moving pedestrian crashes). Independent variables related to direct visibility were indicators for driver-side blind zone size for the left-turning pedestrian crash analysis only (> 20% and ≤ 30% vs. ≤ 20%, > 30% vs. ≤ 20%), passenger-side blind zone size for the right-turning pedestrian crash analysis only (> 50% and ≤ 65% vs. ≤ 50%, > 65% vs. ≤50%), front NVP distance (> 6m and ≤ 9 m vs. ≤ 6 m, > 9 m vs. ≤ 6 m), and front FOV width (> 85° and ≤ 90° vs. >90° , ≤ 85° vs. > 90°). Categories were defined based on the quartile values of these measurements for a 50th percentile male driver. Categorized measurements instead of the actual numbers were used because some values on the low and high ends could potentially skew the analysis results.

Other independent variables included indicators for area type (urban vs. rural), speed limits (30–35 mph vs. ≤ 25 mph, 40–50 mph vs. ≤ 25 mph, ≥ 55 mph vs. ≤ 25 mph), weather (rain/snow/fog/wind/other vs. no adverse conditions), light conditions (dark vs. day, dawn/dusk vs. day), driver and pedestrian sex (female vs. male), driver ages (16–19 vs. 20–29, 30–49 vs. 20–29, 50–69 vs. 20–29, 70+ vs. 20–29), and pedestrian ages (16–19 vs. 20–69, 70+ vs. 20–69).

Estimated coefficients of these independent variables were used to calculate changes in the odds of left-turning or right-turning pedestrian crashes (relative to straight-moving pedestrian crashes) associated with direct visibility metrics and other factors. Variables with p values less than 0.05 were considered statistically significant.

2.3.2 Effects of vehicle front structures on direct visibility metrics

Linear regression was performed to examine the effects of A-pillar width, side-mirror size, and front-end geometries on the driver- and passenger-side blind zone sizes separately, with the blind zone size as the dependent variable. Another liner regression analysis was performed to examine the effects of front-end geometries on the front NVP distance, with the front NVP distance as the dependent variable. Both the 50th percentile male and the 5th percentile female driver measurements were examined. Analysis data were organized by vehicle make, series, and model year; a unique combination of vehicle make, series, and model year was one data record.

In the models for blind zone size, independent variables included driver-side A-pillar width (for the driver-side blind-zone-size model only), passenger-side A-pillar width (for the passenger-side blind-zone-size model only), hood leading edge height, hood length, hood angle, windshield angle, and side mirror maximum height and maximum width. The independent variables of the front NVP distance model were hood leading edge height, hood length, hood angle, and windshield angle. Variables with p values less than 0.05 were taken as statistically significant.

3. RESULTS

3.1 Direct visibility metrics

Among the 766 unique combinations of vehicle make, series, and model year of which the 50th percentile male driver measurements were available, there were 257 cars, 50 minivans and large vans, 127 pickups, and 332 SUVs. The 728 combinations of vehicle make, series, and model year with the 5th percentile female measurements included 244 cars, 50 minivans and large vans, 121 pickups, and 313 SUVs. A summary of the direct visibility measurements is shown in Table 1.

Table 1. Summary of direct visibility measurements of all unique combinations of vehicle make, series, and model year, for the 50th percentile male and 5th percentile female drivers

	N [a]	Minimum	First quartile	Median	Third quartile	Maximum	Mean
50th percentile male drivers							
Driver-side blind zone size (%)	766	14.3	22.6	25.7	30.0	51.0	26.8
Passenger-side blind zone size (%)	766	28.1	49.0	54.6	64.1	84.1	56.6
Front NVP distance (m)	766	4.3	6.4	7.5	8.9	15.8	7.8
Front FOV width (deg)	766	56.0	83.4	87.6	92.9	106.7	88.2
5th percentile female drivers							
Driver-side blind zone size (%)	728	17.8	27.5	30.4	37.8	57.3	33.1
Passenger-side blind zone size (%)	728	35.7	66.2	73.2	78.3	97.8	71.9
Front NVP distance (m)	728	4.1	7.4	8.6	10.4	22.6	9.0
Front FOV width (deg)	728	72.6	83.8	87.5	92.2	117.2	87.9

[a] The totals differed for the 50th percentile male and 5th percentile female due to missing measurements.

Direct visibility characteristics varied by driver group and vehicle type (Table 2). The 5th percentile female drivers had larger average blind zone sizes and longer front NVP distances than the 50th percentile males, while the front FOV widths were similar between the two driver groups.

For the 50th percentile male drivers, cars had the largest driver-side blind zones on average while pickups had the smallest; pickups had the largest passenger-side blind zones and the longest front NVP distance on average while minivans and large vans had the smallest; cars and minivans and large vans had similar and wider front FOVs than pickups and SUVs.

For the 5th percentile female drivers, the average blind zones on both the driver and passenger sides were the largest among pickups and the smallest among cars and minivans and large vans. The average front NVP distance was the longest for pickups and the shortest for minivans and large vans. Cars had wider front FOVs on average than the other passenger vehicle types.

Table 2. Means of direct visibility measurements by vehicle type, of all unique combinations of vehicle make, series, and model year, for the 50th percentile male and 5th percentile female drivers

	Cars		Minivans and large vans		Pickups		SUVs	
	N[a]	Mean	*N*[a]	Mean	*N*[a]	Mean	*N*[a]	Mean
50th percentile male drivers								
Driver-side blind zone size (%)	257	29.0	50	26.1	127	24.5	332	26.0
Passenger-side blind zone size (%)	257	54.6	50	50.1	127	63.2	332	56.7
Front NVP distance (m)	257	7.2	50	6.4	127	9.5	332	7.9
Front FOV width (deg)	257	90.6	50	90.4	127	86.1	332	86.8
5th percentile female drivers								
Driver-side blind zone size (%)	244	30.7	50	29.5	121	36.9	313	33.9
Passenger-side blind zone size (%)	244	68.4	50	69.0	121	79.3	313	72.1
Front NVP distance (m)	244	8.1	50	7.8	121	11.3	313	9.0
Front FOV width (deg)	244	90.9	50	87.7	121	86.8	313	86.0

[a] The number of vehicles differed for the 50th percentile male and 5th percentile female due to missing measurements.

3.2 Pedestrian crashes involving left-turning passenger vehicles

A total of 4,493 crashes were included in the analysis, of which 1,539 were left-turning pedestrian crashes and 2,954 were straight-moving pedestrian crashes as the reference. Logistic regression modeling results of the odds of a left-turning pedestrian crash relative to a straight-moving pedestrian crash are shown in Table 3. We used the direct visibility metrics for the 50th percentile male driver in the model estimation.

For the driver-side blind zones, a large (> 30%) and a medium size (> 20% and ≤ 30%) were associated with significant increases of 69.7% and 59.0% in the odds left-turning pedestrian crashes, respectively, when compared with a small size (≤ 20%). A small front FOV width (≤ 85°) was associated

with a significant 50.8% increase in the odds, and a medium front FOV width (> 85° and ≤ 90°) was associated with a significant 18.2% increase in the odds, when compared with a large front FOV width (> 90°). A long front NVP distance (> 9 m) was associated with a significant 36.8% increase in the odds, compared with a short front NVP distance (≤ 6 m); a medium front NVP distance (> 6 and ≤ 9 m) was associated with a nonsignificant 9.8% increase in the odds.

Among other factors the analysis controlled for, relative to straight-moving pedestrian crashes, left-turning pedestrian crashes were more likely to occur in urban than in rural areas and in adverse weather conditions, such as rain and snow, and less likely to occur on roads with higher speed limits and in dark or dawn/dusk light conditions. Female drivers and drivers older than 29 years were associated with higher odds of left-turning pedestrian crashes, but the increases were not always significant. A female pedestrian was more likely to be struck by a left-turning vehicle than a male pedestrian. Compared with pedestrians ages 20–69, younger pedestrians (16–19 years old) were less likely to be involved in left-turning crashes, while older pedestrians (70 years and older) were more likely to be involved. Only the effect for the younger pedestrians was significant.

Table 3. Logistic regression modeling results of the odds of a left-turning pedestrian crash relative to a straight-moving pedestrian crash

Parameter		Estimate	Estimated change in odds	*p* value
Intercept		−1.7561		<.0001
Driver-side blind zone size [a]	>20% and ≤30% vs. ≤20%	0.4635	59.0%	0.0008
	>30% vs. ≤20%	0.5289	69.7%	0.0010
Front FOV width [a]	>85° and ≤90° vs. >90°	0.1668	18.2%	0.0433
	≤85° vs. >90°	0.4107	50.8%	<.0001
Front NVP distance [a]	>6 and ≤9 m vs. ≤ 6 m	0.0939	9.8%	0.3893
	>9 m vs. ≤ 6 m	0.3134	36.8%	0.0063
Area type	Urban vs. rural	0.5218	68.5%	<.0001
Speed limit	30–35 mph vs. ≤25 mph	−0.1204	−11.3%	0.1141
	40–50 mph vs. ≤25 mph	−0.9505	−61.3%	<.0001
	≥55 mph vs. ≤25 mph	−2.1282	−88.1%	<.0001
Weather	Rain/snow/fog/wind/other vs. dry	0.4649	59.2%	<.0001

Parameter		Estimate	Estimated change in odds	*p* value
Light condition	Dark vs. daylight	−0.6866	−49.7%	<.0001
	Dawn/dusk vs. daylight	−0.3576	−30.1%	0.0243
Driver sex	Female vs. male	0.1225	13.0%	0.0766
Pedestrian sex	Female vs. male	0.7472	111.1%	<.0001
Driver age	16–19 vs. 20–29	0.1010	10.6%	0.5996
	30–49 vs. 20–29	0.1531	16.5%	0.1100
	50–69 vs. 20–29	0.2028	22.5%	0.0421
	70+ vs. 20–29	0.2207	24.7%	0.0717
Pedestrian age	16–19 vs. 20–69	−0.4277	−34.8%	0.0006
	70+ vs. 20–69	0.0924	9.7%	0.3951

[a] The 50th percentile male driver measurements were used.

3.3 Pedestrian crashes involving right-turning passenger vehicles

A total of 3,505 crashes were included in the analysis, of which 575 were right-turning pedestrian crashes and 2,930 were straight-moving pedestrian crashes. Table 4 presents the logistic regression modeling results of the odds of a right-turning pedestrian crash relative to a straight-moving pedestrian crash. We used the direct visibility measurements for the 50th male driver.

Direct visibility metrics had small associations with right-turning pedestrian crashes that were not statistically significant. The estimated effects of road, environment, and pedestrian- and driver-related factors on the odds of right-turning pedestrian crashes were similar to their effects on the odds of left-turning pedestrian crashes as described earlier, except driver sex. Female drivers were less likely to be involved in right-turning pedestrian crashes than male drivers.

Table 4. Logistic regression modeling results of the odds of a right-turning pedestrian crash relative to a straight-moving pedestrian crash

Parameter		Estimate	Estimated change in odds	*p* value
Intercept		−1. 5075		<.0001
Passenger-side blind zone size [a]	>50% and ≤65% vs. ≤50%	−0.0073	−0.7%	0.9512
	>65% vs. ≤50%	−0.0860	−8.2%	0.5488
Front FOV width [a]	>85° and ≤90° vs. >90°	−0.0872	−8.4%	0. 4532
	≤85° vs. >90°	0.0853	8.9%	0.4668
Front NVP distance [a]	>6 and ≤9 m vs. ≤ 6 m	−0.1212	−11.4%	0.3531
	>9 m vs. ≤ 6 m	−0.0386	−3.8%	0.8271
Area type	Urban vs. rural	0.3756	45.6%	0.0017
Speed limit	30–35 mph vs. ≤25 mph	0.0175	1.8%	0.8758
	40–50 mph vs. ≤25 mph	−0.0321	−3.2%	0.8060
	≥55 mph vs. ≤25 mph	−1.3323	−73.6%	0.0002
Weather	Rain/snow/fog/wind/other vs. dry	0.2929	34.0%	0.0488
Light condition	Dark vs. daylight	−1.3154	−73.2%	<.0001
	Dawn/dusk vs. daylight	−0.6638	−48.5%	0.0038
Driver sex	Female vs. male	−0.2084	−18.8%	0.0323
Pedestrian sex	Female vs. male	0.4888	63.0%	<.0001
Driver age	16–19 vs. 20–29	0.1443	15.5%	0.5948
	30–49 vs. 20–29	0.2296	25.8%	0.0971
	50–69 vs. 20–29	0.3140	36.9%	0.0270
	70+ vs. 20–29	0.1961	21.7%	0.2597
Pedestrian age	16–19 vs. 20–69	−0.8344	−56.6%	<.0001
	70+ vs. 20–69	0.0941	9.9%	0.5232

[a] The 50th percentile male driver measurements were used

3.4 Effects of vehicle front structures on blind zone sizes and front NVP distance

The blind zone sizes and front NVP distances obtained by using the camera-based transformation method for both the 50th percentile male and 5th percentile female drivers were examined. The estimated effects of vehicle structures were not always consistent between the driver groups.

3.4.1 Driver-side blind zone sizes

For the 50th percentile male drivers, an increase in the driver-side A-pillar width measured at the driver's eye-height horizon increased the driver-side blind zone size, while for the 5th percentile female drivers, it reduced the driver-side blind zone size (Table 5). Both effects were statistically significant. A higher hood leading edge and a longer hood increased the blind zone, and a larger windshield angle reduced the blind zone size for both driver groups. An increase in the hood angle increased the blind zone size for 50th percentile male drivers and reduced the blind zone size for 5th percentile female drivers, but the effect for the 5th percentile female drivers was not statistically significant.

An increase in the maximum width of the side mirror significantly increased the blind zone size for both driver groups, with a much larger effect size for the 5th percentile female drivers than for the 50th percentile male drivers. A side mirror with a larger maximum height significantly increased the blind zone for 5th percentile female drivers, but did not have an effect for the 50th percentile male drivers.

Table 5. Linear regression modeling results of the effects of vehicle front-structure geometries on driver-side blind zone sizes

Parameter	50th percentile male drivers		5th percentile female drivers	
	Estimate	*p* value	Estimate	*p* value
Intercept	8.2363	<.0001	0.5666	0.8813
Driver-side A-pillar width (deg)	0.4109	<.0001	−0.1941	0.0415
Hood leading edge height (in.)	0.2538	<.0001	0.1735	0.0292
Hood length (in.)	0.0483	0.0619	0.2568	<.0001
Hood angle (deg)	0.0994	0.0054	−0.1109	0.0705
Windshield angle (deg)	−0.1783	<.0001	−0.3180	<.0001
Side mirror maximum height (cm)	0.0066	0.9149	0.4077	0.0002
Side mirror maximum width (cm)	0.1478	0.0164	1.1225	<.0001

3.4.2 Passenger-side blind zone sizes

An increase in the passenger-side A-pillar width at a driver's eye height significantly reduced the passenger-side blind zone size for 50th percentile male drivers, and was associated with a nonsignificant increase in the passenger-side blind zone size for 5th percentile female drivers (Table 6). Estimated effects of hood leading edge height, hood length, and windshield angle on passenger-side blind zone sizes were similar to their effects on driver-side blind zone sizes. Hood angle did not have a significant effect on the passenger-side blind zone size for both driver groups.

An increase in the maximum width of the side mirror was associated with significant increases in the passenger-side blind zone sizes for both driver groups, and the effect size was larger for the 5th percentile female drivers than for the 50th percentile male drivers. An increase in the maximum height of the side mirror was associated with a reduction in the blind zone size for 50th percentile male drivers and an increase for 5th percentile female drivers, but both effects were not statistically significant.

Table 6. Linear regression modeling results of the effects of vehicle front-structure geometries on passenger-side blind zone sizes

Parameter	50th percentile male drivers		5th percentile female drivers	
	Estimate	*p* value	Estimate	*p* value
Intercept	36.5166	<.0001	22.1103	0.0001
Passenger-side A-pillar width	−1.1224	<.0001	0.1470	0.5085
Hood leading edge height (in.)	0.3598	0.0015	0.3615	0.0009
Hood length (in.)	0.4429	<.0001	0.4312	<.0001
Hood angle (deg)	−0.0029	0.9735	−0.0301	0.7225
Windshield angle (deg)	−0.1880	0.0089	−0.2408	0.0006
Side mirror maximum height (cm)	−0.0225	0.8824	0.2727	0.0665
Side mirror maximum width (cm)	0.3383	0.0233	1.0257	<.0001

3.4.3 Front NVP distance

Taller hood leading edges and longer hoods significantly increased the front NVP distance for both driver groups (Table 7). An increase in the hood angle reduced the front NVP distance for the 50th percentile male drivers and increased the front NVP distance for the 5th percentile female drivers, and the effect for the 5th percentile female drivers was not statistically significant. A larger windshield angle significantly reduced the front NVP distance for both driver groups.

Table 7. Linear regression modeling results of the effects of vehicle front-structure geometries on front NVP distance

Parameter	50th percentile male drivers		5th percentile female drivers	
	Estimate	*p* value	Estimate	*p* value
Intercept	0.7352	0.2972	−2.0486	0.0253
Hood leading edge height (in.)	0.1381	<.0001	0.2132	<.0001
Hood length (in.)	0.1010	<.0001	0.1300	<.0001
Hood angle (deg)	−0.0238	0.0544	0.0208	0.1916
Windshield angle (deg)	−0.0512	<.0001	−0.0738	<.0001

4. DISCUSSION

This is the first known study that examined if passenger vehicles with certain driver direct visibility characteristics such as larger blind zones were overrepresented in turning pedestrian crashes. A camera-based transformation method was used to quantify drivers' direct visibility to the front and sides and accounted for obscuration by all vehicle front structures. The findings show that larger driver-side blind zones, longer front NVP distances, and narrower front FOVs were associated with increased risks of left-turning pedestrian crashes, relative to straight-moving pedestrian crashes. The study also validated the effects of vehicle front structures including A-pillars, side mirrors, hoods, and windshields on blind zone sizes.

The finding on the relationship between the driver-side blind zone size and left-turning pedestrian crash risk was consistent with Jagtap and Jermakian (2025). However, the current left-turning pedestrian crash results suggest that the driver-side blind zone sizes alone did not fully capture the effects of driver direct visibility on crash risks, which were also significantly affected by the front NVP distance and front FOV width. A longer distance between a driver and the NVP in front would make pedestrians more likely to enter the front blind zone. A driver in a left-turning vehicle might not be able to perceive and react to a partially blocked adult pedestrian in front in time to avoid a crash, as opposed to a driver in a straight-moving vehicle, who would be able to see a pedestrian from further down the road before a pedestrian enters the front blind zone. A wider front FOV moves the high-obscuration zones further away from the vehicle travel path and makes it easier for a driver to see a pedestrian (Ogawa et al., 2013; Reed, 2008).

No significant effects of direct visibility metrics were found on the risk of right-turning pedestrian crashes. This is consistent with Jagtap and Jermakian (2025), which found that crossing pedestrians were barely in blind zones in right-turning scenarios. Another possible reason for this finding is that when drivers turn right on red or at a stop/yield sign, they tend to focus more of their attention on the conflicting vehicle traffic coming from the left and pay less attention to the right side where there may be pedestrians or bicyclists (Summala et al., 1996; Wu & Xu, 2017). As a result, many of the right-turning

pedestrian crashes might have occurred due to drivers failing to look to the right, instead of pedestrian obscuration. Hu and Cicchino (2022) also found that the odds of right-turning pedestrian crashes relative to straight-moving pedestrian crashes did not differ significantly between cars and larger passenger vehicles.

Multiple vehicle structures affect drivers' direct visibility to the front and side. While previous research on passenger-vehicle blind zones mainly focused on A-pillar geometries (Allen et al., 2001; Ogawa et al., 2013; Santos et al., 2020; Sivak et al., 2007), this study found that in addition to A-pillars, windshield angle, side-mirror size, and front-hood geometry all contributed to blind zone sizes, and the estimated effects of some structures differed by driver group (50th percentile male vs. 5th percentile female). Hood leading edge height, hood length, and windshield angle had effects consistent between the two driver groups. The side-mirror maximum width and height had larger sizes of effects on the blind zone sizes for 5th percentile female drivers than for 50th percentile male drivers. A possible reason is that due to their height and seat position, the 5th percentile female driver's eyes were closer to the side mirrors both vertically and horizontally than the 50th percentile male driver's eyes. As a result, the side mirrors would be a more up-close obstruction of view for the 5th percentile female drivers. The estimated effects of A-pillar width measured at a driver's eye-height horizon were mixed and not always significant. For example, a wider A-pillar at a driver's eye height increased the driver-side blind zone size for the 50th percentile male drivers and reduced the driver-side blind zone size for the 5th percentile female drivers. In many vehicles, A-pillars do not remain a consistent width from top to bottom. Instead, they broaden on the bottom. A 5th female driver's eyes may tend to be near the base of A-pillars while a 50th percentile male driver' eyes may be near the top of A-pillars in smaller vehicles. These findings suggest that when evaluating direct visibility on the driver and passenger sides, we should not rely solely on A-pillar width measured at the horizon of a certain height, which does not account for A-pillar shape nor for obscuration by other structures such as hoods and side mirrors.

The study findings on the effects of various direct visibility metrics provided some insight into increased left-turning pedestrian crash risk associated with larger passenger vehicles such as SUVs and pickups, as Hu and Cicchino (2022) found. Among vehicles included in this study, while the average 50th percentile male driver-side blind zone size was larger among cars than pickups and SUVs, the average front FOV width was larger for cars than for pickups and SUVs for 50th percentile male drivers. Also, pickups and SUVs had longer average front NVP distance than cars. By assuming a car, a SUV, and a pickup with direct visibility measurements equal to the mean values within each vehicle type as shown in Table 2, based on the modeling results (Table 3), the estimated odds of a left-turning pedestrian crash relative to a straight-moving pedestrian crash was 47.2% higher for the pickup and 18.2% higher for the SUV than for the car, given that all the other factors were of the same value. The pattern of the 5th percentile female driver-side blind zone sizes by passenger vehicle type differed from the 50th percentile male drivers: pickups and SUVs had larger blind zones on average than cars and minivans and large vans for the 5th percentile female drivers. The difference in direct visibility between the two driver groups could be attributed to differences in driver eye positions, as discussed earlier.

It is worth noting that categories of direct visibility metrics created in the crash analysis and direct visibility statistics by vehicle type presented in the paper were based on vehicles included in this study only. They may not apply to the entire vehicle fleet, especially not to newer vehicles in the fleet. Most of the vehicles in this study were older models, and vehicle design has been continuously evolving. Epstein et al. (2025) examined the forward blind zones of six popular passenger vehicle models across several redesign cycles during 1997 to 2023 and found blind zones of all the vehicles grew over time. The direct visibility metrics were measured by using maps of NVPs at ground level and did not account for pedestrian heights. However, since all the vehicles were measured by using the same approach at ground level, the study findings would still be valid by focusing on the relative differences between categories for each visibility metric.

Based on the study findings, there are vehicle design changes that automakers could make to improve drivers' direct visibility, including reducing the width of A-pillars, making A-pillars less sloped, moving A-pillars further apart, reducing side-mirror sizes, lowering front ends, and reducing hood length. Side-view cameras can be used to expand drivers' view surrounding the vehicle and minimize blind zones (Beresnev et al., 2018). Modifications to vehicle front structures such as lower and sloped front ends, more space between the hood and engine, and hood airbags can also reduce pedestrian injury severity (Hu et al., 2024; Strandroth et al., 2014). There are rating systems of direct visibility for heavy trucks in the United Kingdom (Transport for London, 2025) and Europe (United Nations Economic Commission for Europe regulation 167), and these heavy vehicles must meet the requirement of a minimum direct vision space around the vehicle to be able to operate. In the United States, methods have been developed to evaluate direct vision for both heavy trucks and passenger vehicles (Brodeur et al., 2023; Drake et al., 2023; Mueller et al., 2025), and a direct vision rating system has been created to provide a self-assessment tool for commercial trucks (Together for Safer Roads, 2025).

AEB systems that can detect pedestrians to mitigate or avoid crashes with them by automatically applying the brakes are another vehicle countermeasure for pedestrian safety. While pedestrian AEB can effectively reduce pedestrian crashes (Cicchino, 2022; Wakeman et al., 2019), these systems were not effective in reducing pedestrian crashes involving a turning vehicle (Cicchino, 2022). Larger safety benefits for pedestrians could be achieved if pedestrian AEB could better detect pedestrians during turning maneuvers, especially for vehicles with poor visibility.

Engineering treatments and road design can also help drivers see pedestrians more easily. For example, a leading pedestrian interval gives pedestrians a head start of a few seconds to enter the crosswalk before vehicles in the parallel direction receive a green light. A curb extension, which extends the curb line into the roadway, positions pedestrians farther ahead of adjacent vehicles. These treatments can help move pedestrians out of blind zones before drivers begin turning.

5. ACKNOWLEDGEMENTS

The authors wish to thank Becky Mueller and Mike Powell from the Insurance Institute for Highway Safety for generating direct visibility metrics. This work was supported by the Insurance Institute for Highway Safety.

6. REFERENCES

Allen, M. J., Abrams, B. S., Ginsburg, A. P., & Weintraub, L. (2001). *Forensic aspects of vision and highway safety*. Lawyers & Judges Publishing Company, Inc. https://books.google.com/books?id=4Ktk5HVvW98C

Ballesteros, M. F., Dischinger, P. C., & Langenberg, P. (2004). Pedestrian injuries and vehicle type in Maryland, 1995–1999. *Accident Analysis & Prevention*, *36*(1), 73–81. https://doi.org/10.1016/s0001-4575(02)00129-x

Beresnev, P. O., Tumasov, A. V., Zeziulin, D. V., Porubov, D. M., & Orlov, L. N. (2018). Development of a detection road users system in vehicle A-pillar blind spots. *IOP Conference Series: Materials Science and Engineering*, *386*(1), 012008. https://doi.org/10.1088/1757-899X/386/1/012008

Brodeur, A., Englin, E., Epstein, A. K., & Vennema, A. (2023). *Boston Blind Zone Safety Initiative: Current fleet analysis, market scan, and proposed direct vision rating framework* (Report No. DOT-VNTSC-BOS-23-01). Volpe National Transportation Systems Center.

Cicchino, J. B. (2022). Effects of automatic emergency braking systems on pedestrian crash risk. *Accident Analysis & Prevention*, *172*, 106686. https://doi.org/10.1016/j.aap.2022.106686

Drake, J., Vennema, A., Slonim, L., Englin, E., Brodeur, A., Epstein, A. K., & Fisher, D. L. (2023). Evaluating the performance of a web-based vehicle blind zone estimation application: Validation and policy implications [Methods]. *Frontiers in Future Transportation*, *4*. https://doi.org/10.3389/ffutr.2023.1003175

Edwards, M., & Leonard, D. (2022). Effects of large vehicles on pedestrian and pedalcyclist injury severity. *Journal of Safety Research*, *82*, 275–282. https://doi.org/10.1016/j.jsr.2022.06.005

Epstein, A., Brodeur, A., Drake, J., Englin, E., Fisher, D. L., Zoepf, S., Mueller, B., & Bragg, H. (2025). Longitudinal analysis of forward blind zone changes in popular vehicle models (1997–2023). *SAE International Journal of Transportation Safety*, *13*(1), 67–78. https://doi.org/10.4271/09-13-01-0005

Federal Highway Administration. (2023). *Proven safety countermeasures*. Retrieved June 2023, from https://highways.dot.gov/safety/proven-safety-countermeasures

Galal, A., Farah, G., Birsen, D., & and Roorda, M. J. (2024). Human factors affecting truck – vulnerable road user safety: A scoping review. *Transport Reviews*, *44*(6), 1209–1234. https://doi.org/10.1080/01441647.2024.2379905

Hu, W., & Cicchino, J. B. (2020a). The effects of left-turn traffic-calming treatments on conflicts and speeds in Washington, DC. *Journal of Safety Research*, *75*, 233–240. https://doi.org/10.1016/j.jsr.2020.10.001

Hu, W., & Cicchino, J. B. (2020b). Lowering the speed limit from 30 mph to 25 mph in Boston: Effects on vehicle speeds. *Injury Prevention*, *26*(2), 99–102. https://doi.org/10.1136/injuryprev-2018-043025

Hu, W., & Cicchino, J. B. (2022). Relationship of pedestrian crash types and passenger vehicle types. *Journal of Safety Research*, *82*, 392–401. https://doi.org/10.1016/j.jsr.2022.07.006

Hu, W., & Cicchino, J. B. (2024). Effects of lowering speed limits on crash severity in Seattle. *Journal of Safety Research*, *88*, 174–178. https://doi.org/10.1016/j.jsr.2023.11.004

Hu, W., Houten, R. V., Cicchino, J. B., Engle, J., & Shomaly, L. A. (2025). Effects of crosswalk illuminators and rectangular rapid flashing beacons on speed reductions and yielding to pedestrians at night. *Transportation Research Record*, *2679*(5), 402–413. https://doi.org/10.1177/03611981241310131

Hu, W., & McCartt, A. T. (2016). Effects of automated speed enforcement in Montgomery County, Maryland, on vehicle speeds, public opinion, and crashes. *Traffic Injury Prevention*, *17 Suppl 1*, 53–58. https://doi.org/10.1080/15389588.2016.1189076

Hu, W., Monfort, S. S., & Cicchino, J. B. (2024). The association between passenger-vehicle front-end profiles and pedestrian injury severity in motor vehicle crashes. *Journal of Safety Research*, *90*, 115–127. https://doi.org/10.1016/j.jsr.2024.06.007

Hussein, W., Tawfeek, M., & Sayed, M. (2017). Investigation of drivers FOV and related ergonomics using laser shadowgraphy from automotive interior. *Journal of Ergonomics*, *07*(4), 1000207. https://doi.org/10.4172/2165-7556.1000207

Insurance Institute for Highway Safety. (2024). *Direct visibility measurement protocol, Version II*.

Insurance Institute for Highway Safety. (2025). Analysis of 2022 data from the Fatality Analysis Reporting System and the Crash Report Sampling System [Unpublished analysis].

Jagtap, S. R., & Jermakian, J. S. (2025). Vehicle blind zones and pedestrian safety at intersections: Identifying high-risk scenarios using mathematical simulations. *Traffic Injury Prevention*. https://doi.org/10.1080/15389588.2025.2520915

Lefler, D. E., & Gabler, H. C. (2004). The fatality and injury risk of light truck impacts with pedestrians in the United States. *Accident Analysis & Prevention*, *36*(2), 295–304. https://doi.org/10.1016/s0001-4575(03)00007-1

Longhitano, D., Henary, B., Bhalla, K., Ivarsson, J., & Crandall, J. (2005). *Influence of vehicle body type on pedestrian injury distribution* (SAE Technical Paper 2005-01-1876). SAE International. https://doi.org/10.4271/2005-01-1876

Monfort, S. S., Hu, W., & Mueller, B. C. (2024). Vehicle front-end geometry and in-depth pedestrian injury outcomes. *Traffic Injury Prevention*, *25*(4), 631–639. https://doi.org/10.1080/15389588.2024.2332513

Monfort, S. S., & Mueller, B. C. (2020). Pedestrian injuries from cars and SUVs: Updated crash outcomes from the Vulnerable Road User Injury Prevention Alliance (VIPA). *Traffic Injury Prevention*, *21*(sup1), S165–S167. https://doi.org/10.1080/15389588.2020.1829917

Mueller, B., Bragg, H., & Bird, T. (2025). Developing a camera-based perspective transformation method for quantifying driver direct visibility for passenger vehicles. WCX 2025 World Congress Experience, Detroit, MI.

Naumann, R. B., West, B. A., Barry, V., Matthews, S., & Lee, R. (2025). Pedestrian and overall road traffic crash deaths — United States and 27 other high-income countries, 2013–2022. *Morbidity and Mortality Weekly Report*, *74*(8), 134–139. https://doi.org/10.15585/mmwr.mm7408a2

Ogawa, S., Chen, Q., Kawaguchi, K., Narikawa, T., Yoshimura, M., & Lihua, S. (2013). Effect of visibility and pedestrian protection performance on pedestrian accidents. *23rd International Technical Conference on the Enhanced Safety of Vehicles (ESV)*, Seoul, South Korea.

Paulozzi, L. J. (2005). United States pedestrian fatality rates by vehicle type. *Injury Prevention*, *11*(4), 232–236. https://doi.org/10.1136/ip.2005.008284

Reed, M. (2008). Intersection kinematics: A pilot study of driver turning behavior with application to pedestrian obscuration by A-pillars (Report No. UMTRI-2008-54). The University of Michigan Transportation Research Institute.

Rothman, L., Macpherson, A., Buliung, R., Macarthur, C., To, T., Larsen, K., & Howard, A. (2015). Installation of speed humps and pedestrian-motor vehicle collisions in Toronto, Canada: A quasi-experimental study. *BMC Public Health*, *15*, 774. https://doi.org/10.1186/s12889-015-2116-4

Roudsari, B. S., Mock, C. N., & Kaufman, R. (2005). An evaluation of the association between vehicle type and the source and severity of pedestrian injuries. *Traffic Injury Prevention*, *6*(2), 185–192. https://doi.org/10.1080/15389580590931680

Roudsari, B. S., Mock, C. N., Kaufman, R., Grossman, D., Henary, B. Y., & Crandall, J. (2004). Pedestrian crashes: Higher injury severity and mortality rate for light truck vehicles compared with passenger vehicles. *Injury Prevention*, *10*(3), 154–158. https://doi.org/10.1136/ip.2003.003814

Santos, A., Gerez, A., Pádua, A., Genaro, P., Silva, R., & Ferreira, S. (2020). *The influence of A-pillar obscuration/location on driver visibility* (SAE Technical Paper 2019-36-0062). SAE International. https://doi.org/10.4271/2019-36-0062

Sivak, M., Schoettle, B., Reed, M. P., & Flannagan, M. J. (2007). Body-pillar vision obstructions and lane-change crashes. *Journal of Safety Research*, *38*(5), 557–561. https://doi.org/10.1016/j.jsr.2007.06.003

Strandroth, J., Sternlund, S., Lie, A., Tingvall, C., Rizzi, M., Kullgren, A., Ohlin, M., & Fredriksson, R. (2014). Correlation between Euro NCAP pedestrian test results and injury severity in injury crashes with pedestrians and bicyclists in Sweden. *Stapp Car Crash Journal*, *58*, 213–231. https://doi.org/10.4271/2014-22-0009

Summala, H., Pasanen, E., Rasanen, M., & Sievanen, J. (1996). Bicycle accidents and drivers' visual search at left and right turns. *Accident Analysis & Prevention, 28*(2), 147–153. https://doi.org/10.1016/0001-4575(95)00041-0

Together for Safer Roads. (2025). *Enhancing road safety through direct vision*. Retrieved June 2025, from https://togetherforsaferroads.org/our-work/direct-vision-star-rating-system/

Transport for London. (2025). *Direct vision standard and HGV safety permit scheme*. Retrieved March 2025, from https://tfl.gov.uk/info-for/deliveries-in-london/delivering-safely/direct-vision-in-heavy-goods-vehicles

Wakeman, K., Moore, M., Zuby, D., & Hellinga, L. (2019). Effect of Subaru EyeSight on pedestrian-related bodily injury liability claim frequencies. *26th International Technical Conference on the Enhanced Safety of Vehicles (ESV)*, Eindhoven, Netherlands.

Wilson, C., Willis, C., Hendrikz, J. K., Le Brocque, R., & Bellamy, N. (2010). Speed cameras for the prevention of road traffic injuries and deaths. *Cochrane Database Systematic Review*, Issue 10, CD004607. https://doi.org/10.1002/14651858.CD004607.pub3

Woolsgrove, C. (2014). ECF report on HGV cabs direct vision and amendments to directive 96/53. European Cyclist Federation.

Wu, J., & Xu, H. (2017). Driver behavior analysis for right-turn drivers at signalized intersections using SHRP 2 naturalistic driving study data. *Journal of Safety Research*, *63*, 177–185. https://doi.org/10.1016/j.jsr.2017.10.010

Young, J., Brodeur, A., Byrne, A., Calabrese, C., Cesic, L., Isaacs, M., Englin, E., Xi, B., Sheehan, T., Yamani, Y., Epstein, A. K., & Fisher, D. L. (2023). Heavy duty truck and pedestrian crashes at signalized intersections: Comparison of high-vision and low-vision cab drivers' performance on a driving simulator. *Transportation Research Record*, *2677*(3), 1123–1136. https://doi.org/10.1177/03611981221121267